AJNR

Functional Connectivity of the Human Red Nucleus in the Brain Resting State at 3T

C. Nioche, E.A. Cabanis and C. Habas

AJNR Am J Neuroradiol 2009, 30 (2) 396-403
doi: https://doi.org/10.3174/ajnr.A1375
http://www.ajnr.org/content/30/2/396

ORIGINAL RESEARCH

Functional Connectivity of the Human Red Nucleus in the Brain Resting State at 3T

C. Nioche
E.A. Cabanis
C. Habas

BACKGROUND AND PURPOSE: Previous structural data obtained with diffusion tensor imaging axonal tracking have demonstrated possible in vivo connections between the human red nucleus (RN) and the sensorimotor and associative cortical areas. However, tractographic reconstructions can include false trajectories because of, for instance, the low spatial resolution of diffusion images or the inability to precisely detect fiber crossings. The rubral network was therefore reassessed by functional connectivity during the brain resting state. Because the RN is located very close to the substantia nigra (SN), the nigral network was also studied to ensure that these 2 circuits were correctly dissociated.

MATERIALS AND METHODS: Data from 14 right-handed healthy volunteers were acquired at rest and analyzed by region-of-interest (ROI)–based functional connectivity. The blood oxygen level–dependent (BOLD) signal intensity fluctuations of separate ROIs located in the RN and SN were successively used to identify significant temporal correlations with BOLD signal intensity fluctuations of other brain regions.

RESULTS: Low-frequency BOLD signal intensity of the RN correlated with signal intensity fluctuations in the cerebellum; mesencephalon; SN; hypothalamus; pallidum; thalamus; insula; claustrum; posterior hippocampus; precuneus; and occipital, prefrontal, and fronto-opercular cortices. Despite some cortical and subcortical overlaps with nigral connectivity, this rubral network was clearly distinct from the nigral network, which showed a strong correlation with the striatum; cerebellar vermis; and more widespread frontal, prefrontal, and orbitofrontal cortical areas.

CONCLUSIONS: During the brain resting state, the human RN participates in cognitive circuits related to salience and executive control, and that may partly represent a subclass of its structural connectivity as revealed by tractography.

In monkeys, the red nucleus (RN) is divided into a small caudoventral magnocellular part and a larger rostrodorsal parvocellular part, which represents approximately 60% to 75% of the nuclear volume.[1] The red nuclear neurons receive afferents from the cerebral cortex on their distal dendrites and from the deep cerebellar nuclei on their proximal dendrites and perikarya. Cerebral cortical axons also terminate on local inhibitory gamma-aminobutyric acid (GABA)ergic interneurons.[2] In more precise terms, the magnocellular RN (mcRN) is mainly connected to the motor and premotor cortices (arm and leg areas) and the cerebellar interposed nuclei.[3,4] The mcRN gives rise to the crossed rubrospinal tract to spinal motor neurons and interneurons of distal, particularly flexor, muscles.[5] Magnocellular neurons showed a movement-related activity that clearly correlated with duration, amplitude, and velocity of independent distal movements.[6,7]

On the contrary, the parvocellular RN (pcRN) receives its main afferents from the primary, frontal, and supplementary motor cortices, which account for 90% of the total corticorubral afferents arising from the cortical sublamina V, and it projects onto the bulbar olivary complex via the central tegmental tract. Parts of the cingulate and parietal cortices (Brodmann area [BA] 24 and 5) also send fibers to the pcRN. Because neurons in pcRN have not displayed any strong movement-related discharges,[8] it has been proposed that this nucleus could be involved in complex motor coordination rather than simple movements or may even be involved in nonmotor functions. The mcRN and rubrospinal tract have markedly regressed from apes to humans[9] so that the human RN mainly consists in its parvocellular part.[1,10]

Streamlining and probabilistic diffusion tensor imaging (DTI) axonal tracking[11,12] have demonstrated extensive cortical afferents to the human RN derived from the prefrontal, pericentral, temporal, and occipital cortices, and subcorticorubral afferents from the dentate and lentiform nuclei in keeping with previous data obtained in leukotomized patients.[13-16] These results also confirmed that the main efferent is represented by the inferior olive. These interconnections between the pcRN and associative cortical areas could suggest a rubral involvement in cognitive functions, especially because the neocerebellum, its main source of afferents, plays a role in cognition and emotion.[17] However, the function of the human RN remains unclear. Clinical studies have provided limited information. An RN infarction was followed by motor symptoms (tremor, asynergia, dysmetria, hypotonia, adiadochokinesis) and cognitive symptoms (intellectual fatigability, decreased verbal fluency, discrete memory impairment),[1,18] but the motor deficiency could be because of a lesion of the superior cerebellar peduncle surrounding the RN, or a lesion of the overlying basal thalamus.[19]

Myoclonic movements have also been described after interruption of the rubro-olivary tract. Rubral neuronal activity in Parkinson disease was increased during passive and voluntary movements.[20] Functional imaging studies have shown that rubral activation correlated with motor performances with a complex rhythm,[21] sensory discrimination,[22] overt speech production,[23] pain processing,[24] and procedural com-

Received July 29, 2008; accepted after revision September 18.

From Service de radiologie (C.N.), Hôpital du Val-de-Grâce, Paris, France; and Service de NeuroImagerie (E.A.C., C.H.), CHNO des Quinze-Vingts, Paris, France.

Please address correpondence to Christophe Habas, MD, Service de NeuroImagerie, CHNO des Quinze-Vingts, UPMC Paris 6, 28 rue de Charenton, 75012 Paris, France; e-mail: chabas@quinze-vingts.fr

DOI 10.3174/ajnr.A1375

plexity,[25] whereas limited correlation was observed during simple movement performance.[22] Thus, because of its connection with the associative cortical and cerebellar cortices, and its possible nonmotor-related activity, as revealed by functional MR imaging (fMRI), the RN may be involved in higher cognitive functions in addition to a weaker role in motor performances. Notwithstanding, the above-mentioned structural and functional results are limited by at least 2 points. First, DTI tractography identifies only possible anatomic connections because false tracking may occur in low-anisotropic areas and because of the usual low spatial resolution of the DTI images, consecutive partial volumes, and the difficulty in detecting fiber crossings. Second, most of the fMRI paradigms have used motor performances and not pure cognitive tasks.

Therefore, to overcome these 2 limitations, we chose to reassess the human rubral network by using functional connectivity MR imaging (fcMRI) in the brain resting state. In brief, this method is based on the existence of temporal correlations between spontaneous low-frequency (0.01–0.1 Hz) fluctuations in the blood oxygen level–dependent (BOLD) signal intensity of remote but functionally related brain areas.[26-28] To determine the brain areas specifically linked with the RN, we applied a region-of-interest (ROI) analysis. This analysis looked for significant correlations between mean BOLD signal intensity fluctuations of a ROI located in the RN and BOLD signal intensity fluctuations of other brain regions. Moreover, as this analysis was carried out at rest, with no overt movement performance, it can be assumed that the resulting corticorubral network would underlie nonmotor cognitive function of the RN. Furthermore, the RN is separated from the substantia nigra (SN) by the tiny ventral tegmental area in the mesencephalon, and nigrorubral projections have been traced in the monkey.[29] Consequently, it was therefore important to ascertain 1) that ROI within the RN did not include parts of the SN, and 2) whether the functional connectivity of the RN and the SN, belonging to the striatal system,[30] was different. Four distinct ROIs located in the right and left RN and in the right and left SN were therefore defined to compare RN-centered and SN-centered circuits.

Materials and Methods

Subjects. This analysis was performed on 14 right-handed healthy subjects (age, 19–40 years; mean age: 26.5 years), all of whom gave their informed consent before the study. These subjects had no history of cardiovascular, neurologic, or psychiatric disease.

Task procedure. Subjects lay supine and still, with closed eyes and both hands extended, in a MR imaging machine (Signa Horizon; GE Healthcare, Milwaukee, Wis) throughout the examination.

fMRI data acquisition. We conducted fMRI on a whole-body 3T clinical imager (Signa Horizon; GE Healthcare) by using an 8-channel head coil. In each scanning sequence, 32 contiguous axial T2*-weighted gradient-echo echo-planar images (TE, 40 ms; TR, 2500 ms; FOV, 30 × 30 mm; matrix, 128 × 128; thickness, 4 mm; intersection spacing, 0 mm; NEX, 1) were obtained to encompass the entire brain and cerebellum. A total of 216 volumes were acquired including 4 "dummy" volumes obtained at the start of the session. Off-line, T2*-weighted images were coregistered and overlaid on their corresponding anatomic IR-weighted gradient-echo images (TE, 3 ms; TI, 450 ms; TR, 7.3 ms; flip angle, 20°; FOV, 25.6 × 25.6 mm; matrix, 256 × 256; thickness, 1 mm; intersection spacing, 0 mm).

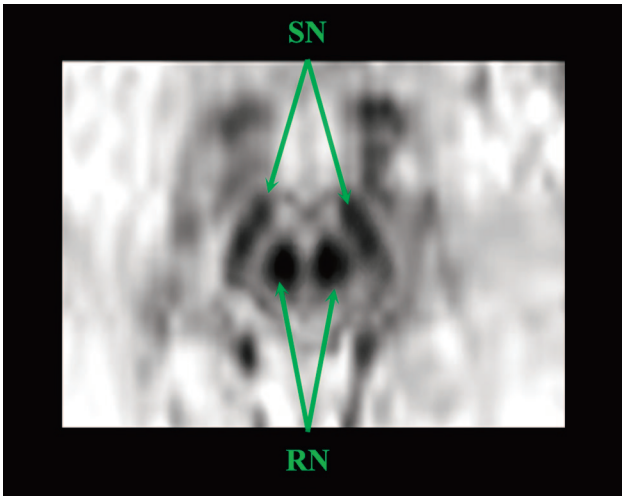

Fig 1. Axial T2*-weighted images through the mesencephalon showing the RN and SN on the right and left sides, with a strong signal hypointensity.

Statistical Analysis

Preprocessing. Functional images were preprocessed and analyzed with use of Statistical Parametric Analysis (SPM5) (http://www.fil.ion.ucl.uk/spm). Data were successively format-converted, motion-corrected, corrected for errors in section-timing, spatially smoothed with a 6-mm full width at half maximum of Gaussian kernel, and coregistered with use of the template brain of the Montreal Neurologic Institute proportional spatial scaling.

ROIs. The red nuclei and SN appear as a strong hypointense signal intensity on T2-weighted images in the mesencephalon so that their borders are easily identifiable (Fig 1). For all subjects and all nuclei, the ROIs were manually drawn (by the same experimenter) to precisely delineate each nucleus (on both sides) on axial T2*-weighted images with use of FSLview (tool of the FMRIB Software Library [FSL. Version 4; Oxford Centre of Functional MR imaging of the Brain, UK; http://www.fmrib.ox.ac.uk/fsl]). For each subject, it was verified that no overlapping existed between red nuclear and nigral ROIs. The ROIs were then format-converted from NIFTI to .mat files with use of the MARSBAR option of SPM5 to carry out functional connectivity analysis.

Functional connectivity analysis. These 2 ROIs were used for separate fcMRI analyses. For each subject, the mean time-series from the task-free scans were extracted from the ROI by averaging the time-series of all voxels in the ROI. To minimize the effect of global drift, we scaled the voxel intensities by dividing the value of each time point by the mean value of the whole-brain image at that point. The resulting time-series was then used as a covariate of interest in a whole-brain, linear regression, statistical parametric analysis. Contrast images corresponding to the ROI time-series regressor were entered into a second-level, random-effects analysis (height and extent thresholds: $P < .01$ and $k = 50$, for significant clusters, corrected at the whole brain) to determine the brain areas that showed functional connectivity across subjects.

Results

Red nuclei. For each nucleus, clusters were observed bilaterally, as shown in Fig 2 and Table 1: prefrontal cortex (BA,

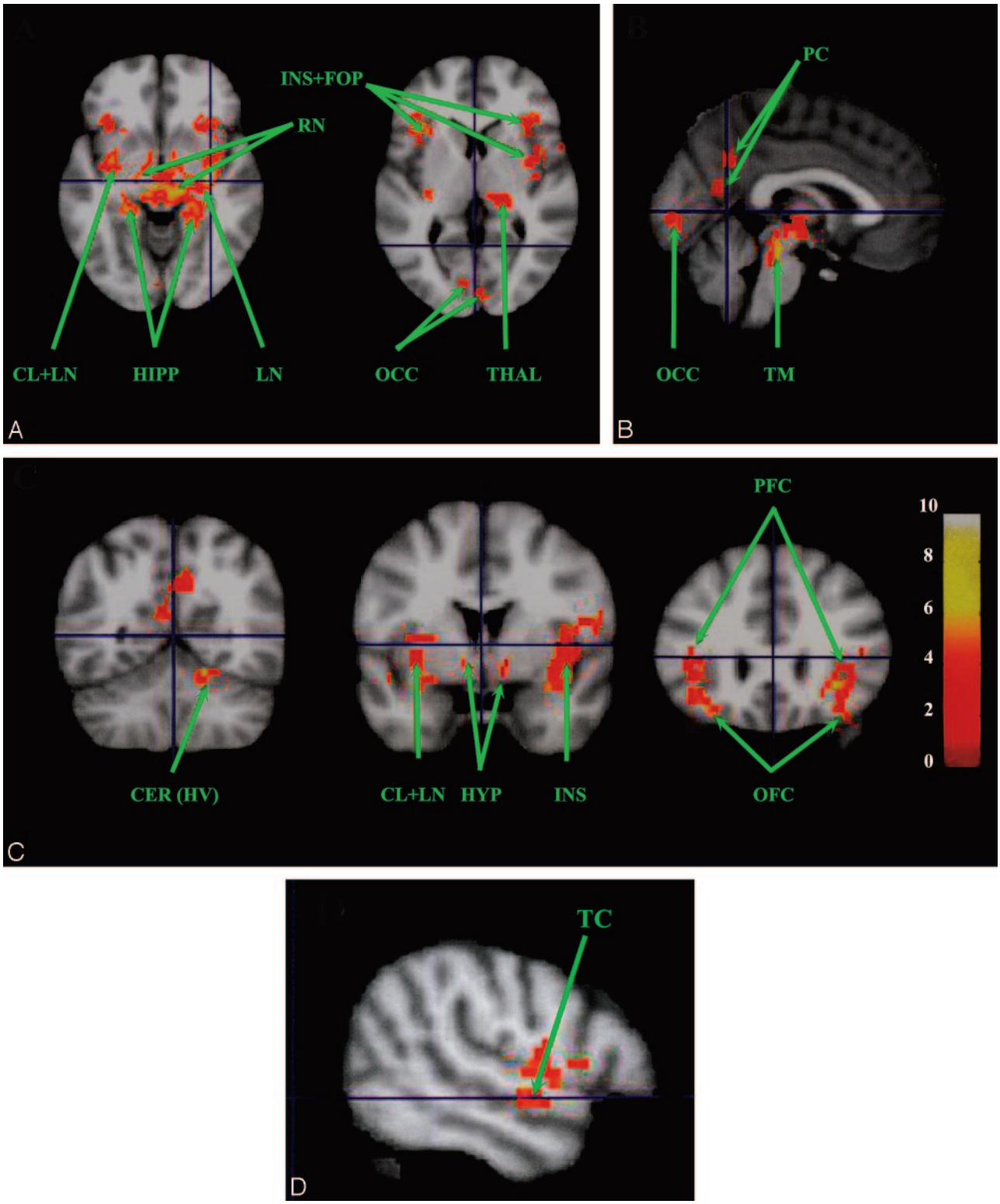

Fig 2. Resting-state neural connectivity maps ($n = 14$; $P < .01$; and k = 50) showing regions positively correlated with the right RN (*A-C*) and also found with the left RN. *A*, Axial sections. *B*, Sagittal section. *C*, Coronal sections. *D*, Sagittal section showing temporal region correlated with the left RN. *D*, T-score is represented by a color gradient (*vertical colored bar*). ACC, anterior cingulate cortex; CL, claustrum; CER, cerebellum; FOP, fronto-opercular cortex; HIPP, hippocampus; HYP, hypothalamus; INS, insula; LN, lentiform nucleus (pallidum and putamen); MES, mesencephalon; PFC, prefrontal cortex; RN, red nucleus; SN, substantia nigra; ST, striatum; THAL, thalamus; TC, temporal cortex; TM, tegmentum of the mesencephalon; m, medial; OFC, orbito-frontal cortex; HV, hemisphere of lobule V; OCC, occipital cortex.

11/45/47), occipital cortex (BA 17/37), posterior hippocampus (BA 35), caudal insula (BA 13), claustrum, ventrolateral and posterior thalamus, posteroinferior pallidum with a possible extension within the contiguous putamen, hypothalamus, contralateral RN, and mesencephalic tegmentum. Clusters were also found in the right and left precuneus (BA 7) for the right RN, anterosuperior temporal gyrus (BA 20), and dorsolateral prefrontal cortex (BA 9) for the left RN, and the right

Table 1: Cluster localizations of the red nuclei

		Group-Analysis p <0.01, k = 50 MNI Coordinates (mm)					
		Primary Peak Locations					
		Right Side			Left Side		
Brain Region	BA	*x*	*y*	*z*	*x*	*y*	*z*
Right red nucleus							
Prefrontal cortex	45 (/47)	35.10	28.08	4.00	–32.76	23.40	–12.00
	11	35.10	28.08	–12.00	–36.11	36.02	–13.54
Precuneus	7 m	6.86	–60.12	34.00	–3.86	–60.12	18.46
Occipital cortex	17	7.02	–86.58	–4.00	00.00	–88.92	4.00
	36	32.76	–39.78	–16.00	–	–	–
Hippocampus	35	23.40	–42.12	–8.00	–21.06	–35.10	–8.00
Insula	13	35.10	–16.38	–4.00	–36.11	–13.42	11.14
Claustrum		32.16	–17.08	–8.00	–33.08	–2.13	–8.05
Thalamus		15.62	–27.16	0.17	–12.86	–27.16	0.17
Hypothalamus		9.60	–1.52	–8.97	–6.43	–1.52	–8.97
Pallidum		14.04	–7.02	–8.00	–18.72	–16.38	00.00
Mesencephalic tegmentum		3.68	–27.16	–16.28	–3.20	–28.99	–11.79
Cerebellum		16.00	–58.50	–16.28	–	–	–
Left red nucleus							
Prefrontal cortex	45 (/47)	35.10	28.08	–8.00	–35.10	28.08	–8.00
	46	–	–	–	–37.44	39.78	12.00
	11	35.10	30.42	–4.00	–32.76	37.44	–12.00
Occipital cortex	37	25.74	–49.14	–12.00	–	–	–
Temporal cortex	20	53.82	–4.68	–8.00	–	–	–
Hippocampus	35	21.06	–35.10	–8.00	–16.38	–35.10	–8.00
Insula	13	44.46	4.68	–4.00	–35.10	14.04	–4.00
Claustrum		30.42	–16.38	–4.00	–28.08	–16.38	00.00
Thalamus		16.38	–21.06	4.00	–9.36	–21.06	4.00
Hypothalamus		9.36	2.34	–8.00	–4.68	–7.02	–12.00
Pallidum		23.10	–14.04	–4.00	–23.10	–16.38	00.00
Mesencephalic tegmentum		9.36	–28.08	–12.00	–7.02	–25.74	–12.00
Cerebellum		20.88	–51.48	–16.52	–	–	–

Note:—BA indicates Brodmann area; MNI, Montreal Neurological Institute.

cerebellum (hemisphere of lobule V) for both red nuclei. The rubral cluster may extend within the SN.

Substantia nigra. For each nucleus, clusters were observed bilaterally, as shown in Fig 3 and Table 2: prefrontal cortex (BA 11/47), premotor and motor cortices (BA 4/6), posterior hippocampus (BA 35), rostral insula (BA 13), claustrum, striatum including the caudate and lentiform nuclei, anteroventral thalamus, hypothalamus, and mesencephalic tegmentum. The prefrontal clusters were more widespread for the right nucleus (BA 8/9/46); clusters were also found in the right temporal (BA 21) and occipital cortices (BA 19/39), right and left anterior (para-) cingulate cortex (BA 24/32), and right pons. For the left nucleus, clusters were also located in the cerebellar vermis (lobules V-VI).

Discussion

Our study of fcMRI confirms, clarifies, and extends our previous structural results concerning the corticorubral network[11,12] showing that, during the brain resting state: 1) the human RN participates in a widespread functional network including associative prefrontal, parietal, occipital, and temporal areas, and limbic areas such as the ventral lentiform nucleus, hypothalamus, and mesencephalic tegmentum; 2) this network does not include motor areas and was not recruited by overt motor performance; and 3) this network can be dissociated from a nigro-centered striatal network despite the anatomic proximity between the RN and SN.

First, the present data agree with previous analyses of human clinical cases reporting possible projections from associative cortices to the RN including the frontal and prefrontal cortices (BA 4/6/8/9/10/45/46/47),[14-16] insula (BA 13), and temporal and parietal cortices.[14] However, we found more limited prefrontal clusters (BA 11/45/46/47), and clusters were also observed in the hippocampus, claustrum, and primary and associative occipital cortices (BA17/3/37). No direct connections between the RN and these brain regions have been previously described. Furthermore, no correlations were detected between the RN and the premotor and sensorimotor cortices, though strong connections between these structures are observed in monkeys and humans.[11,12] To reconcile all these results, we can test the hypothesis that part of our data reflect sources or targets of direct rubral afferents or efferents, especially those for which tractography revealed anatomic relationships,[11,12] whereas the other part consists of areas encompassed in the functional network centered on the RN, though as-yet-unknown anatomic connections cannot be ruled out. This must be the case for the thalamus, as no rubrothalamic projections exist in the monkey.[31] Absence of "activation" of the premotor and sensorimotor cortices could therefore be ascribed to their absence of recruitment and to the correlative reallocation of the functional connectivity to areas more specifically engaged in the brain resting state.

Although it appears difficult to precisely define the role of the RN in this study, 2 points must be emphasized. The RN is

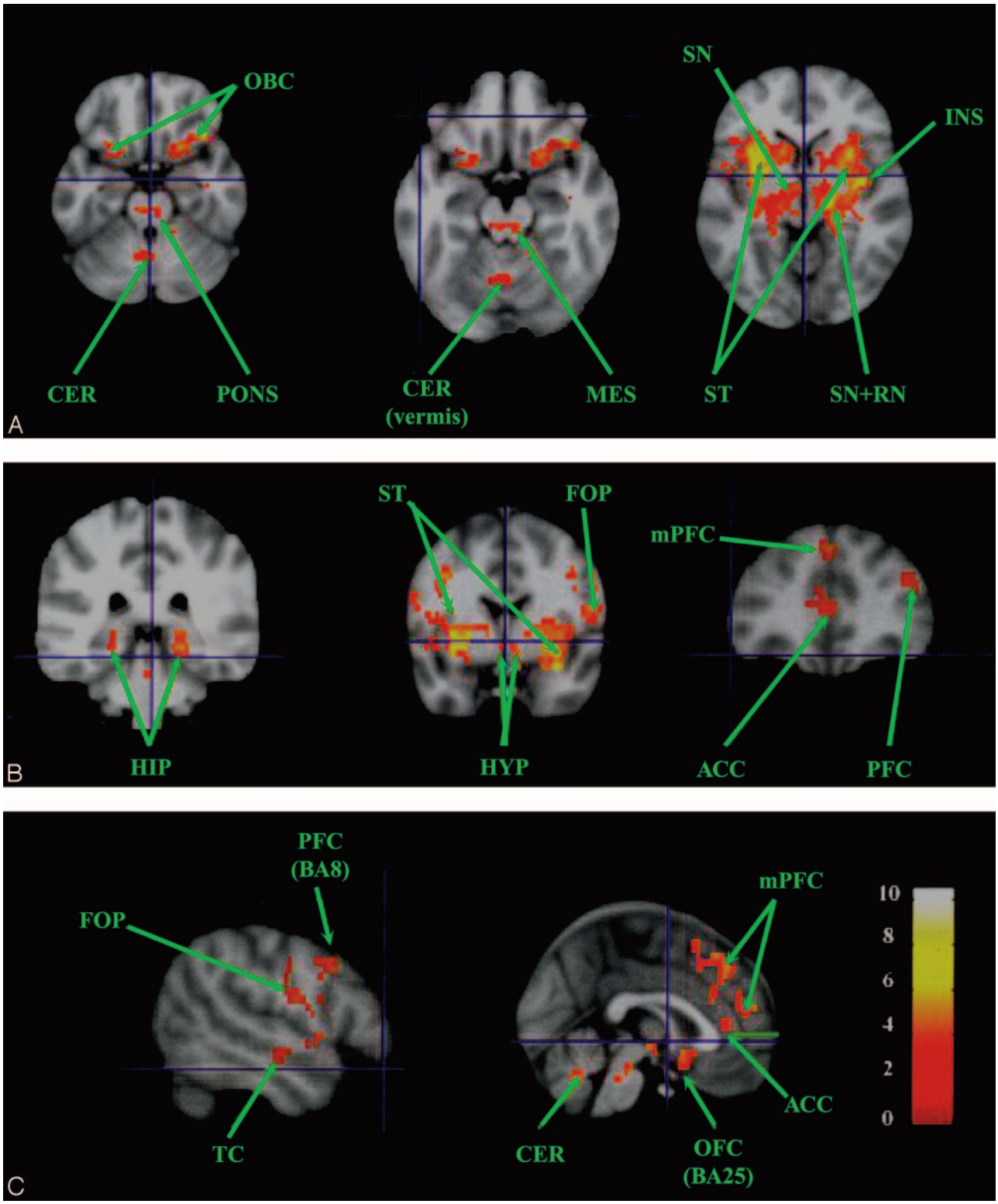

Fig 3. Resting-state neural connectivity maps ($n = 14$; $P < .01$; and $k = 50$) showing regions positively correlated with the left SN (most of them are also found with the right SN; Table 2). *A,* Axial sections. *B,* Coronal sections. *C,* Sagittal sections. T-score is represented by a color gradient (*vertical colored bar*).

exclusively functionally associated with cortical areas devoted to cognitive function such as vision or mental imagery (occipital cortex); emotion (cortex orbitofrontal BA 11 and insula); episodic memory (hippocampus BA 35 and precuneus); working memory, episodic and semantic memory, and reasoning (prefrontal cortex BA 45/46/47); consciousness; mental imagery; and agency (precuneus and insula).[30,32,33] These cortical areas participate in at least 2 well-known networks specific for the brain resting state: the salience network (orbitofrontal, fronto-opercular, and insular cortices)[34] and the default-mode network (precuneus and hippocampus).[35,36] It can be speculated that these associative regions may exert a

Table 2: Cluster localizations of the substantia nigra group-analysis $P < .01$, k = 50 MNI coordinates (mm)

		Brain Region					
		Primary Peak Locations					
		Right Side			Left Side		
BA		*x*	*y*	*z*	*x*	*y*	*z*
Left substantia nigra							
Prefrontal cortex	11/47	37.44	28.08	–4.00	–32.76	28.08	–8.00
Frontal cortex	6 m	11.70	11.70	48.00	–7.02	2.34	48.00
	4	46.80	–7.02	44.00	–	–	–
Orbitofrontal cortex	25	4.68	9.36	–16.00	–2.34	9.36	–13.00
Occipital cortex	19/39	44.46	–79.56	32.00	–	–	–
Temporal cortex	21	53.82	–11.70	–12.00	–51.48	–16.38	–8.00
Hippocampus	35	21.06	–35.10	–12.00	–16.38	–39.78	–12.00
Insula	13	44.46	4.68	–4.00	–30.42	9.36	–4.00
Lentiform nucleus		28.08	11.70	–4.00	–28.08	14.04	00.00
Thalamus		16.38	–16.38	00.00	–11.70	–18.72	4.00
Hypothalamus		7.02	–2.34	–12.00	–2.34	–2.34	–16.00
Mesencephalic tegmentum		4.68	–30.42	–20.00	–4.68	–28.08	–16.00
Pons		00.00	–32.76	–24.00	–	–	–
Right substantia nigra							
Prefrontal cortex	46	46.80	39.78	20.00			
	11 (/47)	32.76	25.74	–8.00	–25.74	23.40	–16.00
	9 (/6)	51.48	18.72	40.00	–	–	–
	8	4.68	37.44	40.00	–2.34	37.44	44.00
Orbitofrontal cortex	25	7.02	9.36	–12.00	–4.68	9.36	–12.00
Motor cortex	4	51.48	–9.36	40.00	–56.16	–4.68	24.00
Cingulate cortex	24 (/32)	8.27	44.26	20.29	–2.34	37.44	8.00
Hippocampus	35	11.70	–39.78	–12.00	–23.40	–25.74	–12.00
Insula	13	39.78	–4.68	8.00	–41.59	11.70	2.00
Lentiform nucleus		25.74	4.68	–4.00	–25.74	11.70	–8.00
Caudate nucleus		9.60	11.30	2.92	–11.70	16.38	00.00
Claustrum		32.76	14.04	–4.00	–32.76	–11.70	–8.00
Thalamus		15.62	–14.34	4.00	–11.03	–16.17	4.00
Hypothalamus		11.70	–4.68	–8.00	–4.68	–4.68	–8.00
Mesencephalic tegmentum		7.02	–30.42	–20.00	–2.34	–28.08	–20.00
Cerebellum (vermis)		11.70	–56.16	–28.00	–4.68	–60.84	–24.00

modulatory action on the olivocerebellar system via the RN, which massively projects to the principal olivary nucleus via the central tegmental tract. It is also tempting to ascribe the cognitive impairments (short- and long-term memory, verbal fluency, intellectual fatigability)[18] observed in patients with rubral lesions to alterations of the cerebello-rubro-olivo-cerebellar loop and, in particular, to the lack of modulatory effect of the rubral afferents on the cognitive and affective cerebellum. In a very unexpected turn, only the right cerebellar anterior lobe (HV) exhibited correlated fluctuations with the right and left red nuclei. A threshold problem may account for this observation as well as the fact that in some volunteers: 1) the dentate nucleus and the very posterior cerebellar lobe were not covered by the sections, and 2) image distortions in the caudal pons and posterior cerebellum from aeration of the sphenoid sinus were present. The anterior cerebellar lobe received inputs from the mediocaudal basilar pontine nucleus,[37] which is interconnected with the hypothalamus and limbic and autonomic cortical areas.[38] This cerebellar region may therefore represent one of the targets of the rubro-olivary system mobilized in the brain resting state and may participate in a limbic/autonomic loop anchored in the RN. It is noteworthy that the inferior olive and cerebellum (HV), and apparently the rubral area, are specifically recruited while encoding temporal information of "unexpected" sensory events.[39] In our study, the RN could constitute a relay for salience detection of affective/autonomic information.

Second, functional connectivity was also found between the RN and subcortical loci (hypothalamus, SN, mesencephalic tegmentum). These results are in keeping with previous data obtained in monkeys[40] and humans,[41] showing connections between the RN and midbrain areas such as the mesencephalic reticular formation, periaqueductal gray matter, superior colliculus, SN, and hypothalamus. It is noteworthy that these structures also belong to the salience network[34] involved in emotional salience processing. Moreover, functional imaging[24] has demonstrated activation in the RN, SN, and periaqueductal gray matter during pain processing, especially the emotive salience of visceral pain. Therefore, the red nuclear activity must be influenced by cortical and subcortical emotional information and may then modulate the cognitive and affective cerebellum[17,38] via the bulbar olivary nucleus or directly via, at least, the interposed nucleus.[41] Correlated BOLD fluctuations within the contralateral RN were also found for each RN and mostly in the bilateral homologous cortical and subcortical regions. This bilaterality can be explained by 1) rubro-rubral fibers passing through the posterior commissure[41] and 2) possible bilateral cortical and subcortical projections, as demonstrated in monkeys for the supplementary motor area.[42]

Third, the rubral network could also have reflected 1) the whole cerebellar system, as its main input originates in the dentate nucleus; and 2) the striatal system as, because of partial volume effects, the ROI may have included part of the SN and as GABAergic[43] nigrorubral projections[29] have been described in animals. Allen et al[44] seeded the dentate nuclei to carry out functional connectivity of the cerebellar system. They found a widespread neural network comprising the prefrontal, temporal, parietal, and occipital cortices; hippocampus; thalamus; hypothalamus; caudate and lentiform nuclei; and cerebellum, but did not report any cluster within the RN. Our rubral circuit may therefore constitute, at rest, a distinct cerebellar subsystem with more limited, though partly overlapping, neural nodes compared with the functional network anchored in the dentate nucleus. This observation reinforces the hypothesis that this rubral circuit may subserve a more focused activity such as detection of salience.

The functional connectivity of the SN also showed a widespread network markedly different from the rubral network, especially with frontal, prefrontal, and orbitofrontal (BA 4/8/9/25), cingulate,[24] and temporal (BA 21) cortices, striatal and anterior vermian relays not present in the rubral circuit. Moreover, our results concerning SN are in agreement with previous data obtained in animals.[30,45-48] The pars reticulata of SN (prSN) participates in a direct cortico-striato-nigro-thalamo-cortical circuit and an indirect cortico-striato-subthalamo-nigro-thalamo-cortical circuit.[30] These circuits are subdivided into motor, limbic, and associative parallel closed loops according to their cortical origins (motor, cingulate and hippocampal, and prefrontal areas, respectively).[49] The pcSN also sends fibers to the superior colliculi and the pedunculopontine tegmental nucleus. The pars compacta of SN (pcSN) participates in a striato-nigro-striatal circuit. More precisely, prSN is connected with the motor cortex, temporal cortex (TE), prefrontal eye field (BA 8), and prefrontal cortex (BA 9/12/46) in monkeys.[47,48] Our in vivo human study confirms these previous observations and shows that these circuits are clearly identifiable during the brain resting state, though it is difficult to clearly distinguish direct and indirect circuits. However, we found a more extensive prefrontal (BA 11/47) "activation" and associative occipital (BA 19/39) and orbitofrontal (BA 25) "activations" not previously reported, as well as vermian recruitment (lobuli V-VI). This subregion of the cerebellum receives hypothalamic, tectal, and perihypoglossal nuclei[30] (visual attention and saccadic movements). The basal ganglia are involved in supervised, rule- and reward-based learning of motor and cognitive habits and also subserve visuospatial and executive functions,[50] so that they could coordinate other cortical networks, such as executive defaults and salience networks,[34,35] activated during the brain resting state. Finally, although nigrorubral connections exist, the rubral and nigral networks remain functionally independent during the brain resting state. At least 2 hypotheses can be proposed: either the inhibitory nigro-rubral projections contribute to decouple rubral and nigral functioning, or the part of the SN linked with the RN is different from the part of the SN included in the striatal loops.

Fourth, some technical points and limitations must be emphasized. We used a TR of 2500 ms, which can cause aliasing because of respiratory- and cardiac-related fluctuations. Moreover, the statistical threshold for significant clusters was fixed at less than 0.01, though it is usually fixed at less than 0.001, increasing the risk for false-positive results. Finally, given the section thickness and the small size of the RN and SN, the partial volume in the selected ROIs may have contributed to errors. Therefore, functional connectivity data must be interpreted with caution. However, as aforementioned, our results were coherent with known anatomy and physiology. Furthermore, the main partial volume error may have concerned the rubral and nigral nuclei, but we showed that the RN-centered and SN-centered networks were clearly distinct. Of course, it cannot be ruled out that small parts of adjacent subcortical structures such as the zona incerta, reticular formation, subthalamic nucleus, and thalamus could have been included in the ROIs. One possibility to address these problems and to verify our results would be to complement our study by a model-free, independent component analysis.[27] This method is well suited to discriminate sources of noise, such as physiologic aliasing, and to identify statistically independent neural networks. Moreover, an unbiased template-matching procedure could be applied to the individual independent component analysis maps, including the RN and SN, to identify previously described intrinsically connected brain networks such as salience and executive control networks.[34]

Conclusions

To our knowledge, this is the first functional connectivity study devoted to the RN and, incidentally, to the SN in humans. During the brain resting state, the RN displays strong functional coherence with associative prefrontal, insular, temporal, and parietal cortices; the thalamus; and the hypothalamus, but not with the sensorimotor cortex. These results support a cognitive role of the RN, probably related to salience detection and executive control. This rubral circuit, which seems to constitute a modular cerebellar subsystem, clearly differs from the striatal loops passing through the very close and anatomically associated SN. Our study also confirms previous results for the SN obtained in monkeys, reporting corticonigral connections with the prefrontal, temporal, and occipital cortices. Finally, our study demonstrates that this fcMRI technique can be successfully applied to small subcortical structures. However, further investigation is warranted to fully elucidate the specific clinical significance of the rubral and nigral networks that have been demonstrated in this preliminary and exploratory study.

Acknowledgments

The authors thank Katie Keller and Daniel N′Guyen (Stanford University, Calif) for technical support.

References

1. Massion J. **The mammalian red nucleus.** *Physiol Rev* 1967;47:383–436
2. Ralston DD. **Corticorubral synaptic organization in *Macaca fascicularis*: a study utilizing degeneration, anterograde transport of WGA-HRP, and combined immuno-GABA-gold technique and computer-assisted reconstruction.** *J Comp Neurol* 1994;350:657–73
3. Humphrey DR, Gold R, Reed DJ. **Sizes, laminar and topographical origins of cortical projections to the major divisions of the red nucleus in the monkey.** *J Comp Neurol* 1984;225:75–94
4. Stanton GB. **Topographical organization of ascending cerebellar projections from the dentate and interposed nuclei in Macaca mulatta: an anterograde degeneration study.** *J Comp Neurol* 1980;190:699–731

5. Miller RA, Strominger NL. **Efferent connections of the red nucleus in the brainstem and spinal cord of the Rhesus monkey.** *J Comp Neurol* 1973;152: 327–45
6. Miller LE, van Kan PL, Sinjjaer T, et al. **Correlation of primate red nucleus discharge with muscle activity during free-form arm movements.** *J Physiol* 1993;469:213–43
7. Larsen KD, Yumiya H. **The red nucleus of the monkey. Topographic localization of somatosensory input and motor output.** *Exp Brain Res* 1980;40:393–404
8. Kennedy PR, Gibson AR, Houk JC. **Functional and anatomic differenciation between parvicellular and magnocellular regions of the red nucleus in monkey.** *Brain Res* 1986;364:124–36
9. ten Donkelaar HJ. **Evolution of the red nucleus and the rubrospinal tract.** *Behav Brain Res* 1988;28:9–20
10. Patt S, Gerhard L, Zill E. **A Golgi study on the red nucleus in man.** *Histol Histopathol* 1994;9:7–10
11. Habas C, Cabanis EA. **Cortical projections to the human red nucleus: a diffusion tensor tractography study with a 1.5-T MRI machine.** *Neuroradiol* 2006; 48:755–62
12. Habas C, Cabanis EA. **Cortical projections to the human red nucleus: complementary results with probabilistic tractography with a 3-T.** *Neuroradiol* 2007; 49:777–84
13. Von Monakow C. **Experimentelle und pathologisch-anatomische Untersuchungen über die Haubenregion, den Schlügel und die Regio subthalamica nebst Beiträge zur Kenntnis frü h erworbener Gross- und Kleinhirndefecte.** *Archiv Psychiat Nervenkr* 1895;27:1–128, 386–478
14. Archambault L. **Les connexions corticales du noyau rouge.** *Nouvelle Iconographie Salpêtrière* 1914–1915;27:188–225
15. Meyer M. **Study of efferent connexions of the frontal lobe in the human brain after leucotomy.** *Brain* 1949;72:265–96
16. Kanki S, Ban T. **Corticofugal connections of the frontal lobe in man.** *Med J Osaka University* 1952;3:201–22
17. Schmahmann JD, Sherman JC. **The cerebellar cognitive affective syndrome.** *Brain* 1998;121:561–79
18. Lefebvre V, Josien E, Pasquier F, et al. **Infarctus du noyau rouge et diaschisis cérébelleux croisé.** *Rev Neurol (Paris)* 1993;149–4:294–96
19. Martinez Perez-Balsa A, Marti-Masso JF, Lopez de Munain A, et al. **'Rubral' tremor after vascular thalamic lesions.** *Rev Neurol (Spain)* 1998;26:80–84
20. Rodriguez-Oroz MC, Rodriguez M, Leiva C, et al. **Neuronal activity of the red nucleus in Parkinson's disease.** *Mov Disorders* 2008;23:908–11
21. Xu D, Liu T, Ashe J, et al. **Role of the olivo-cerebellar system in timing.** *J Neurosci* 2006;26:5990–95
22. Gao JH, Parsons LM, Bower JM, et al. **Cerebellum implicated in sensory acquisition and discrimination rather than in motor control.** *Science* 1996;272: 545–47
23. Sörös P, Sokoloff LG, Bose A, et al. **Clustered functional MRI of overt speech production.** *NeuroImage* 2006;32:376–87
24. Dunckley P, Wise R, Fairhust M, et al. **A comparison of visceral and somatic pain processing in the human brainstem using functional magnetic resonance imaging.** *J Neurosci* 2005;25:7333–41
25. Liu Y, Pu Y, Gao JH, et al. **The human red nucleus and lateral cerebellum in supporting roles for sensory information processing.** *Hum Brain Mapp* 2000;10:147–59
26. Biswal B, Yetkin FZ, Haughton VM, et al. **Functional connectivity in the motor cortex of resting brain using echo-planar MRI.** *Magn Reson Med* 1995;34: 537–41
27. Fox MD, Raischle ME. **Spontaneous fluctuations in brain activity observed with functional magnetic resonance imaging.** *Nat Rev Neurosci* 2007;8:700–11
28. Greicius M. **Resting-state functional connectivity in neuropsychiatric disorders.** *Cur Opin Neurol* 2008;21:424–30
29. Carpenter MB, Stevens GH. **Structural and functional relationships between deep cerebellar nuclei and brachium conjunctivum in the rhesus monkey.** *J Comp Neurol* 1957;107:109–64
30. Nieuwenhuys R, Voogt J, vanHuijzen C. (eds). *The Human Central Nervous System. A Synopsis and Atlas. 2008*. Fourth revised ed. Berlin: Springer-Verlag; 2008.
31. Hopkins DA, Lawrence DC. **On the absence of a rubrothalamic projection in the monkey with observations on some ascending mesencephalic projections.** *J Comp Neurol* 1975;161:269–94
32. Cabeza R, Nyberg L. **Imaging cognition. II: an empirical review of 275 PET and fMRI studies.** *J Cogn Neurosci* 2000;12:1–47
33. Cavanna AE, Trimble MR. **The precuneus: a review of its functional anatomy and behavioural correlates.** *Brain* 2006;129:564–83
34. Seeley WW, Menon V, Schartzberg AF, et al. **Dissociable intrinsic connectivity networks for salience processing and executive control.** *J Neurosci* 2007;27: 2349–56
35. Greicius MD, Krasnow B, Reiss AL, et al. **Functional connectivity in the resting brain: A network analysis of the default mode hypothesis.** *Proc Natl Acad Sci U S A* 2003;100:253–58
36. Bukner RL, Andrews-Hanna JR, Schacter DL. **The brain's default network. Anatomy, function, and relevance to disease.** *Ann NY Acad Sci* 2008;1124:1–38
37. Schmahmann JD, Pandya DN. **The cerebrocerebellar system.** *Intern Rev Neurobiol* 1997;41:31–60
38. Haines DE, Dietrichs E, Mihailoff GA, et al. **The cerebellar-hypothalamic axis: basic circuits and clinical observations.** *Intern Rev Neurobiol* 1997;41:83–100
39. Liu T, Xu D, Ashe J, et al. **Specificity of inferior olive response to stimulus timing.** *J Neurophysiol* 2007;100:1557–61
40. Hartmann-von Monakow K, Akert K, Künze H. **Projections of precentral and premotor cortex to the red nucleus and other midbrain areas in Macaca fascicularis.** *Exp Brain Res* 1979;34:91–105
41. Foix C, Nicolesco J. *Les noyaux gris centraux et la region mésencéphalo-sous optique.* Paris: Masson; 1925:581
42. Courville J, Brodal A. **Rubro-cerebellar connections in the cat: an experimental study with silver impregnation method.** *J Comp Neurol* 1966;126:471–85
43. Fu YS, Tseng GF, Yin HS. **Extrinsic inhibitory innervation to rubral neurons in rat brain-stem slices.** *Exp Neurol* 1996;137:142–50
44. Allen G, McColl R, Barnard H, et al. **Magnetic resonance imaging of cerebellar-prefrontal and cerebellar-parietal functional connectivity.** *NeuroImage* 2005; 28:39–48
45. Goldman-Rakic PS, Selemon LD. **New frontiers in basal ganglia research.** *Trends Neurosci* 1990;13:241–44
46. Alexander GE, Crutcher MD. **Functional architecture of basal ganglia circuits: neural substrates of parallel processing.** *Trends Neurosci* 1990;13:266–71
47. Middleton FA, Strick PL. **The temporal lobe is a target lobe of output from the basal ganglia.** *Proc Natl Acad Sci U S A* 1996;93:8683–87
48. Middleton FA, Strick PL. **Basal-ganglia 'projections' to the prefrontal cortex of the primate.** *Cereb Cortex* 2002;12:926–35
49. Middleton FA, Strick PL. **Basal ganglia and cerebellar loops: motor and cognitive circuits.** *Brain Res Brain Res Rev* 2000;31:236–50
50. Doya K. **Complementary roles of basal ganglia and cerebellum in learning and motor control.** *Curr Opin Neurobiol* 2000;10:732–39